Finite element modelling of creep cavity filling by solute diffusion

Versteylen, C. D.; Szymański, N. K.; Sluiter, M. H.F.; van Dijk, N. H.

DOI
10.1080/14786435.2017.1418097

Publication date
2018

Document Version
Final published version

Published in
Philosophical Magazine (London, 2003)

Philosophical Magazine

ISSN: 1478-6435 (Print) 1478-6443 (Online) Journal homepage: http://www.tandfonline.com/loi/tphm20

Finite element modelling of creep cavity filling by solute diffusion

C. D. Versteylen, N. K. Szymański, M. H. F. Sluiter & N. H. van Dijk

To cite this article: C. D. Versteylen, N. K. Szymański, M. H. F. Sluiter & N. H. van Dijk (2018): Finite element modelling of creep cavity filling by solute diffusion, Philosophical Magazine, DOI: 10.1080/14786435.2017.1418097

To link to this article: https://doi.org/10.1080/14786435.2017.1418097

Published online: 04 Jan 2018.

PHILOSOPHICAL MAGAZINE, 2018
https://doi.org/10.1080/14786435.2017.1418097

Taylor & Francis
Taylor & Francis Group

Finite element modelling of creep cavity filling by solute diffusion

C. D. Versteylen[a,b], N. K. Szymański[a], M. H. F. Sluiter[b] and N. H. van Dijk[a]

[a]Fundamental Aspects of Materials and Energy, Faculty of Applied Sciences, Delft University of Technology, Delft, The Netherlands; [b]Virtual Materials and Mechanics, Department of Materials Science and Engineering, Delft University of Technology, Delft, The Netherlands

ABSTRACT

In recently discovered self healing creep steels, open-volume creep cavities are filled by the precipitation of supersaturated solute. These creep cavities form on the grain boundaries oriented perpendicular to the applied stress. The presence of a free surface triggers a flux of solute from the matrix, over the grain boundaries towards the creep cavities. We studied the creep cavity filling by finite element modelling and found that the filling time critically depends on (i) the ratio of diffusivities in the grain boundary and the bulk, and (ii) on the ratio of the intercavity distance and the cavity size. For a relatively large intercavity spacing 3D transport is observed when the grain boundary and volume diffusivities are of a similar order of magnitude, while a 2D behaviour is observed when the grain boundary diffusivity is dominant. Instead when the intercavity distance is small, the transport behaviour tends to a 1D behaviour in all cases, as the amount of solute available in the grain boundary is insufficient. A phase diagram with the transition lines is constructed.

ARTICLE HISTORY
Received 17 October 2017
Accepted 12 December 2017

KEYWORDS
FEM; modelling; creep; precipitation; steel; self-healing

1. Introduction

When metals are subjected to a load at high temperature, creep damage can occur in the form of creep cavities. These cavities grow under the influence of stress which can lead to failure. Generally, strategies are adopted to prevent creep damage to form, or slow down its growth [1,2]. An alternative method in the form of self healing has been proposed by Laha and coworkers [3] and Shinya [4], where selective precipitation of supersaturated solute at creep cavities hinders the creep cavity growth in stainless steels. This mechanism was modelled by Karpov and coworkers [5]. Zhang and coworkers subsequently demonstrated that precipitation of substitutional solute leads to the self healing of creep cavities in Fe–Au and Fe–Mo alloys [6–8]. The creep defects and repairing precipitates were studied in detail for Fe–Au self-healing creep alloys, using

CONTACT C. D. Versteylen c.d.versteylen@tudelft.nl

X-ray nanotomography [9]. It was found that the creep cavity growth and the precipitate growth directly affect the strain rate of the alloys. Additional scanning electron microscopy studies indicated a close similarity between the precipitation mechanism at the outer surface [10], compared to the precipitation on the creep cavity surface within the material [9].

Creep cavity growth by the diffusional flux of vacancies over grain boundaries has been described by Herring [11], and Hull and Rimmer [12], who propose that the driving force for vacancies to migrate to the creep cavities is a function of the applied stress. The effect of strain rate in the bulk material on the creep cavity growth was treated in finite-element calculations by Needleman and Rice [13]. The role of stress states around creep cavities, and the effect of the intercavity distance implemented in the model proposed by Needleman and Rice was investigated by van der Giessen [14]. In all of these studies, the vacancy transport is solely along the grain-boundary, by grain-boundary diffusion.

Zener first treated the bulk-diffusion dominated growth of spherical precipitates in a homogeneous bulk material [15]. In the case of precipitate growth on grain-boundaries, both the diffusivity in bulk and on the grain-boundary play an essential role. The fast diffusion along grain boundaries acts as a collector plate to accumulate solute [16], or diffuse solute in the case of precipitate dissolution [17,18].

The aim of the present paper is to quantitatively estimate the time required to fill a creep cavity by solute precipitation as a function of several key modelling parameters such as: the creep cavity size, the intercavity spacing, the concentration of supersaturated solute, the grain-boundary diffusivity and the volume diffusivity. We also aim to show the influence of the diffusivities and intercavity distance on the 1D, 2D or 3D character of the diffusion field and therefore its influence on the rate of filling. The growth rate of a precipitate can change character during the life-time of a material. This change of character can play a significant role in the behaviour of creep-resistant alloys, as they have long service lives at high temperature.

2. Methods

The diffusional flux of substitutional solute towards the creep cavity is evaluated using finite element modelling (FEM). The modelling was performed using the Sepran software [19,20]. The diffusional flux $\vec{J}$ is modelled as,

$$\vec{J} = -\frac{D}{\Omega}\vec{\nabla}c, \tag{1}$$

where D is the diffusion constant, Ω is the atomic volume and c is the solute concentration in atomic fraction. Assuming that the driving force for diffusion originates only from a gradient in concentration ($\vec{\nabla}c$), and that the atomic volume of the solute atom is equal to the volume of an iron atom in the bcc

lattice (Ω). The diffusional flux of solute towards the volume of a lens-shaped cavity is evaluated at the surface of the cavity S:

$$\frac{\mathrm{d}N}{\mathrm{d}t} = -\oiint_S \vec{J} \cdot \vec{dS}. \tag{2}$$

The diffusional flux arriving at the creep-cavity surface S results in a number of ingressing atoms N per unit of time t. The precipitate then grows inside the creep cavity until the number of atoms that have ingressed is sufficient to fill the volume V of the original creep cavity ($N\Omega = V$). The fraction of filling f then corresponds to $f = N\Omega/V$ (with $f = 1$ at complete filling).

As indicated in Figure 1, the simulation volume is a cylinder of radial dimension r and vertical dimension z. The simulation box has a radius λ and a box height H. The grain boundary thickness amounts to $\delta = 0.5$ nm, the creep cavity radius is chosen to be $a = 50$ nm and the atom volume of bcc iron is $\Omega = 0.0117\,\mathrm{nm}^3$ (for a lattice parameter of 0.286 nm).

The boundary conditions are: (1) the concentration at the edge of the creep cavity ($r = a$) is kept at a constant level c_1, (2) the starting concentration in the matrix and grain boundary is chosen to be equal to the nominal concentration c_0 and (3) at the edge of the simulation box ($r = \lambda$ and $z = H$), the diffusional flux is chosen to be zero. The box radius λ corresponds to half the intercavity spacing on the grain boundary ($z = 0$). A small box radius therefore corresponds to a high cavity concentration on the grain boundary. The box height H, was chosen to always be sufficiently large, so that the concentration remains equal to the nominal concentration at the vertical box edge, for the times up until complete filling.

The ratio λ/a is a characteristic parameter in the modelling of the creep cavity filling. In our simulations we used the following values for the intercavity ratios: $\lambda/a = 2, 3, 5, 10, 20, 50, 100, 200$ and 400. We varied the grain-boundary diffusivity (D_{gb}) over 9 orders of magnitude and the volume diffusivity D_V in the bulk of the matrix over 10 orders of magnitude. The shape of the cavities on grain edges, corners and on precipitates has been analysed by Raj & Ashby [21]. The creep cavities that form on the grain boundaries are found to be self-similar over a large range of length scales. In this work, we will only consider the lens-shaped cavities forming on straight grain-boundary edges perpendicular to the stress direction. For such a lens-shaped cavity, the volume is given by $V_{cav} = FV_{sphere}$ with

$$F = 1 - \frac{3}{2}\cos(\psi) + \frac{1}{2}\cos^3(\psi), \tag{3}$$

where ψ is the opening angle and $V_{sphere} = 4\pi a^3/3$ is the volume of a sphere with radius a. For metals the equilibrium opening angle ψ is estimated at 75°, following the approach by Raj and Ashby [21], resulting in a scale factor of $F \approx 0.62$. The height of the creep cavity directly scales with the cavity radius a with $h/a = (1 - \cos\psi)/\sin(\psi) \approx 0.77$.

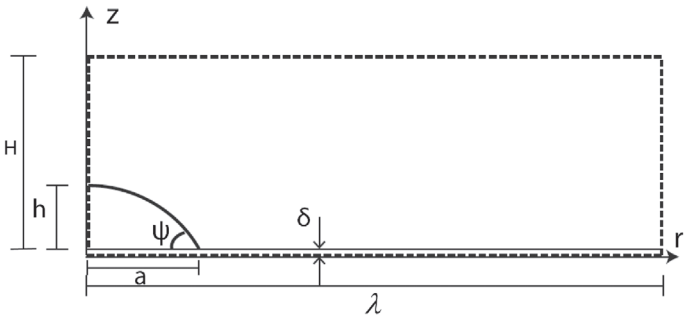

Figure 1. Lens-shaped creep cavity defined by an opening angle ψ, a height h and a radius a. The creep cavity is formed on a grain boundary with width δ. The simulation box is a cylinder with a radius λ and a height H.

Throughout the simulations the nominal concentration is chosen to be $c_0 = 0.01$, with an edge concentration of $c_1 = 0.0001$, in order to reflect the experimental situation for self healing in Fe–Au alloys [6,7,9]. As a consequence, the supersaturation Δc is comparable to the nominal concentration c_0.

3. Results

In Figure 2 the concentration profile at the time of creep cavity filling is shown for $\lambda/a = 20$ and $\lambda/a = 2$, and for three different ratio's of D_{gb}/D_V. It can be seen that the character of the diffusional field where the solute is depleted critically depends on both diffusivity and size ratio. The axially symmetric cavity can have either a 3D, 2D or 1D diffusion field, depending on λ/a and D_{gb}/D_V. For the ratio of $\lambda/a = 2$ the diffusion field has a 1D character with a concentration gradient towards the grain boundary and the creep cavity. For the ratio of $\lambda/a = 20$, the diffusion field has a 3D character for $D_{gb}/D_V \approx 1$, and a 2D character for $D_{gb}/D_V \gg 1$.

In Figure 3, the filling time of the creep cavity as a result of the diffusional solute flux towards the creep cavity is shown as a function of the grain-boundary diffusivity and the volume diffusivity, for different ratio's of λ/a. For the smallest ratio of $\lambda/a = 2$, the filling time is only controlled by D_V. This is consistent with the results of Figure 2, where the diffusion field always shows a 1D character for $\lambda/a = 2$. For $\lambda/a = 5$ and $\lambda/a = 20$, in Figure 3, a clear transition is observed for a specific ratio of diffusivities. For a relatively high grain-boundary diffusion, the grain boundary is depleted faster, leading to a 1D diffusion for most of the filling time. For $\lambda/a = 400$, both the grain boundary and volume diffusivity control the filling time.

Based on these observations it is useful to introduce a dimensionless time τ:

$$\tau = \frac{D_V t}{a^2}. \tag{4}$$

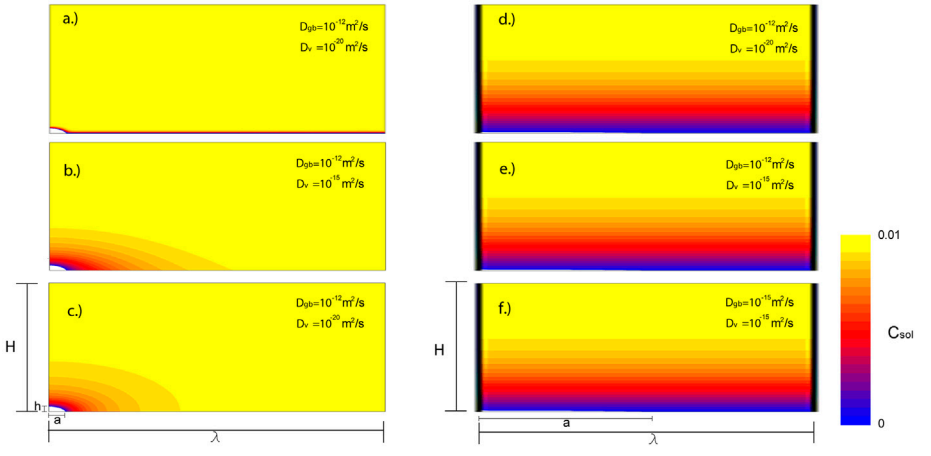

Figure 2. (colour online) Solute concentration around the cavity at the time of filling. (a) $\lambda/a = 20$, and $D_{gb}/D_V = 10^8$. (b) $\lambda/a = 20$, and $D_{gb}/D_V = 10^3$. (c) $\lambda/a = 20$, and $D_{gb}/D_V = 1$. (d) $\lambda/a = 2$, and $D_{gb}/D_V = 10^8$. (e) $\lambda/a = 2$, and $D_{gb}/D_V = 10^3$. (f) $\lambda/a = 2$, and $D_{gb}/D_V = 1$. All data are for a supersaturation of $\Delta c = 0.01$. For $\lambda/a = 2$, the grain boundary contains insufficient solute, and as a result, a quasi-1D profile is observed at the time of filling, independent of the ratio D_{gb}/D_V.

In Figure 4, τ_{fill} is shown for different ratio's of λ/a. For the 1D and 3D conditions, where the volume diffusion is rate-limiting, the dimensionless filling time τ_{fill} is now independent of the volume diffusion D_V. For large values of λ/a, τ_{fill} is also independent of λ/a. For a large ratio of λ/a and $D_{gb}/D_V = 1$, the diffusion field has a 3D character. However, when the grain-boundary diffusivity is much larger than the volume diffusivity $D_{gb} \gg D_V$, the diffusion field shows a distinct 2D character. In Figure 5, the dimensionless filling time (τ_{fill}) is plotted as function of the geometric ratio (λ/a) and the diffusivity ratio (D_{gb}/D_V). τ_{fill} is found to depend on both the ratio of diffusivities and the geometric ratio. For $\lambda/a > 50$ only the diffusivity ratio defines the dimensionless filling time. In this case, for high diffusivity ratios τ_{fill} scales as $t_{fill} \propto \left(D_{gb}/D_V\right)^{-1}$, as t_{fill} is then controlled by D_{gb} only.

The diffusion profile can be 3D, 2D or 1D in nature. In order to evaluate which of these occurs, one can use the diffusion length at the filling $2\sqrt{Dt_{fill}}$. When the diffusion length for grain-boundary and/or volume diffusion exceeds the box radius λ, a cross-over in behaviour occurs. In order to further evaluate the nature of the diffusion process, the amount of atoms ingressing in the creep cavity as function of time can approximated by a power law;

$$N(t) = Kt^{\nu}, \tag{5}$$

where N is the number of solute atoms collected in the cavity, K is a constant and ν is the time exponent, which can be obtained by fitting the simulation results

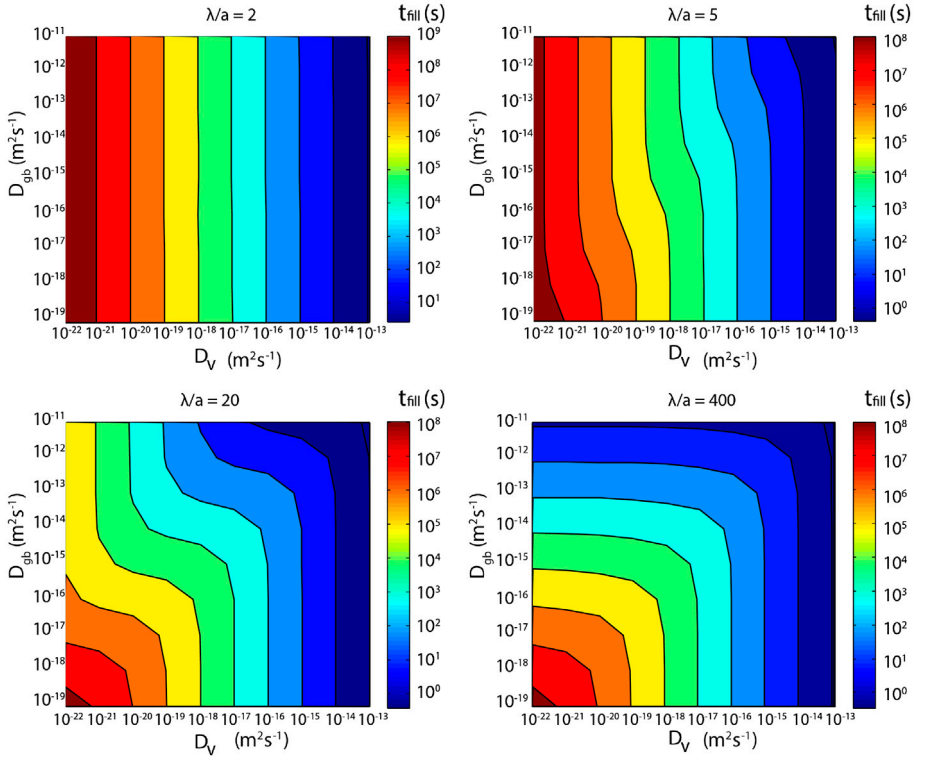

Figure 3. (colour online) Filling time for different ratio's of λ/a (2, 5, 20, 400). The filling time depends only on the volume diffusivity for small λ/a, and evolves to the situation where both diffusivities contribute. All data are for a supersaturation level of $\Delta c = 0.01$.

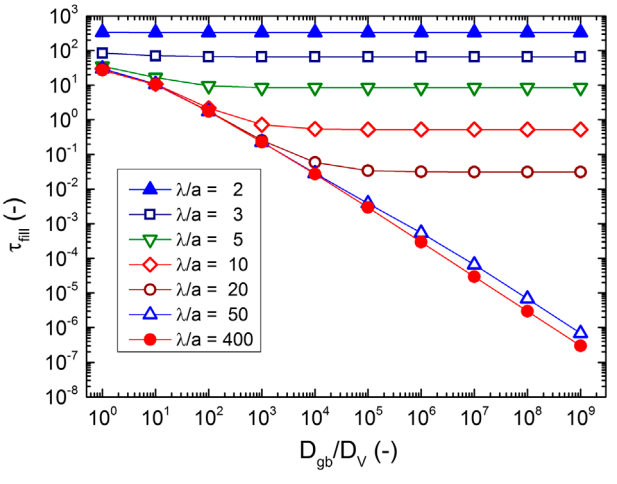

Figure 4. (colour online) Dimensionless filling time τ_{fill}, as function of the diffusivity ratio D_{gb}/D_V. The ratio λ/a defines at which diffusivity ratio the diffusion length impinges the edge of the box at $r = \lambda$. All data are for a supersaturation of $\Delta c = 0.01$.

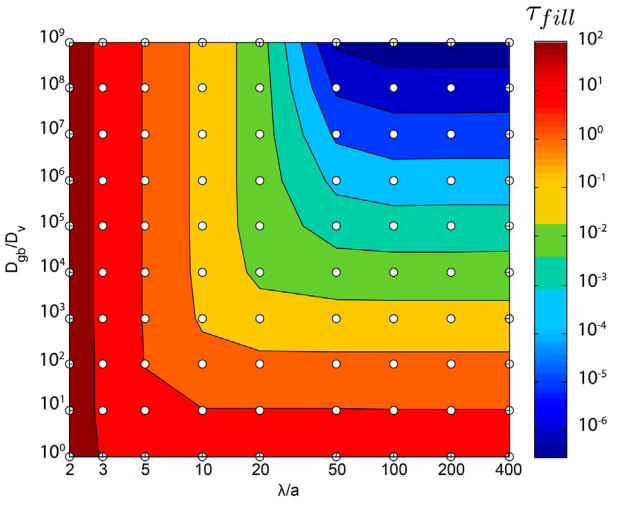

Figure 5. (colour online) Dimensionless filling time τ_{fill} as a function of λ/a and D_{gb}/D_V. All data are for a supersaturation of $\Delta c = 0.01$.

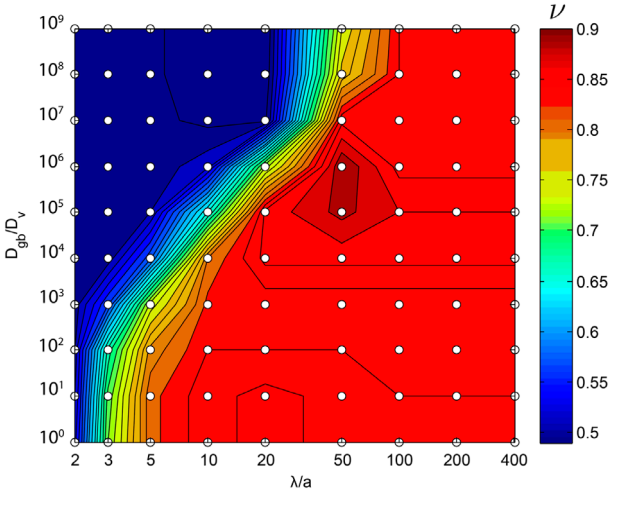

Figure 6. (colour online) Time exponent ν for cavity filling kinetics as a function of λ/a and D_{gb}/D_V. All data are for a supersaturation of $\Delta c = 0.01$.

for $N(t)$ to Equation (5). $N(t)$ is obtained by integrating the atom flux from Equation (2).

The time exponent for the filling kinetics of the creep cavity depends on the dimensional character: for 1D one finds $\nu = 0.5$, and for both 2D and 3D ν starts at 0.5 and gradually tends to 1.0 over time (see Appendix 1). As shown in Figure 6, a 1D character ($\nu = 0.5$) is observed for low values of λ/a, while a 2D/3D character (with $\nu \approx 0.85$) is observed for high values of λ/a. This is consistent with the result from Figures 2–5.

4. Discussion

The dimensional character of the solute transport towards the cavity has a large effect on the filling time. For a small λ/a ratio the solute transport is purely 1D and is controlled by the diffusivity through the bulk towards the grain boundary and creep cavity. The diffusion length required for filling, can be estimated from the grain-boundary surface area (scaling as $S \propto \lambda^2$). The resulting 1D diffusion length $2\sqrt{D_V t_{fill}}$ scales as $V/S\Delta c$, where the volume of the creep cavity scales as $V \propto a^3$. This leads to a dimensionless filling time of $\tau_{fill} \propto (\lambda/a)^{-4}\Delta c^{-2}$. This scaling behaviour can be observed for small λ/a in Figure 4.

For larger λ/a ratios, the filling time depends on D_{gb}/D_V. When $D_{gb} = D_V$, the filling of the creep cavity takes on a 3D character. When the creep cavity is assumed to be spherical, the exact solution for the solute flux on the creep cavity boundary at $r = a$ is (see Appendix 1):

$$J(r = a) = \frac{D_V \Delta c}{a}\left(1 + \frac{1}{\sqrt{\pi\,\tau}}\right). \tag{6}$$

The filling fraction then corresponds to $f(\tau) = 3\Delta c\left(\tau + \sqrt{\frac{4\tau}{\pi}}\right)$. The second term represents the quasi-1D behaviour for short times ($f \propto \sqrt{\tau}$), and the first term refers to the behaviour at large times ($f \propto \tau$). Based on the long-time contribution the dimensionless time to filling can be approximated as $\tau_{fill} \approx \frac{1}{3\Delta c}$.

When the diffusivity ratio D_{gb}/D_V increases ($D_{gb}/D_V \gg 1$), while the inter-cavity distance λ is large enough to provide the solute required to fill the cavity from the grain boundary ($\lambda/a \gg 1$), the diffusion is of 2D character. This means that the filling time depends only on the grain-boundary diffusivity and the grain-boundary width. For 2D diffusional behaviour, the grain-boundary diffusivity is rate controlling, with a time exponent $\nu \approx 1$. A dimensionless filling time of the following form is now expected;

$$\tau_{fill} \propto \frac{1}{\Delta c}\frac{aD_V}{\delta D_{gb}}. \tag{7}$$

In Figure 4, it is clear that only the grain-boundary diffusivity D_{gb} plays a role in filling, then $\tau_{fill} \propto D_V/D_{gb}$. For those cases where grain-boundary diffusion is dominant until impingement occurs (such as in $\lambda/a = 5, 10,$ or 20), the 2D character of filling changes after impingement to 1D. After impingement, the value of τ_{fill} becomes constant.

In Figure 7 the nature of the transport behaviour is indicated as function of λ/a and D_{gb}/D_V. For a high λ/a ratio, and for $D_{gb}/D_V = 1$, the character of the solute transport is 3D. When the diffusivity ratio D_{gb}/D_V increases, the character changes to 2D, which is reflected by the cross-over in Figure 5. For a small λ/a ratio, an increase in the ratio D_{gb}/D_V, leads to a fast impingement. This leads to a 1D character, where the filling time only depends on the volume

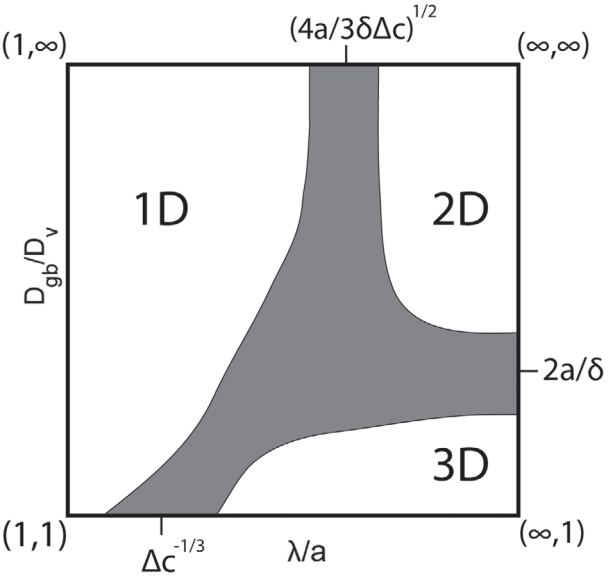

Figure 7. Phase diagram for the diffusional character of creep cavity filling by supersaturated solute, as a function of the diffusivity ratio D_{gb}/D_v and the characteristic length scale ratio λ/a. 3 different regimes with 1D, 2D and 3D diffusion are observed. The characteristic values for the cross-over between these regimes are indicated.

diffusivity. This is clearly indicated by the change in time exponent ν in Figure 6. The phase diagram of Figure 7, schematically summarises the results of Figures 5 and 6. In order to predict the type of behaviour, we can estimate the transition points between 1D, 2D and 3D behaviour. For $\lambda/a \gg 1$ a cross-over between 2D and 3D behaviour is expected when the flux through the grain boundary surface connecting the cavity $S_{gb} = 2\pi a\delta$ and the flux through the bulk surface connecting the cavity $S_V \approx 4\pi a^2$ are balanced. From the flux balance $D_{gb}S_{gb} = D_V S_V$ a transition is expected for $D_{gb}/D_V \approx 2a/\delta$. For the present model parameters this cross-over takes place at $2a/\delta = 200$. In the isotropic limit where $D_{gb} = D_V$, a cross-over is expected when the solute-depleted region impinges with the box radius λ. Assuming for simplicity a complete depletion, a mass balance gives $\frac{4}{3}\pi a^3 = \Delta c \frac{4}{3}\pi\lambda^3$ with a transition between the 1D and 3D character for $\lambda/a \approx \Delta c^{-1/3}$. For $\Delta c = 0.01$, this corresponds to $\lambda/a \approx 4.6$. For $D_{gb}/D_V \gg 1$ a cross-over is expected when the solute depleted region impinges with the box radius λ. Assuming for simplicity a complete depletion a mass balance, then, results in $\frac{4}{3}\pi a^3 = \Delta c\delta\pi\lambda^2$ with a transition between the 1D and 2D character for $\lambda/a \approx \sqrt{\frac{4a}{3\delta\Delta c}}$. For our simulation parameters this occurs at $\lambda/a \approx 115$.

Precipitate growth inside a creep cavity is very similar to the heterogeneous precipitate growth on a grain boundary. The difference between the case analysed here and heterogeneous growth of precipitates on grain boundaries is in the moving boundary. If the boundary is not static, the analysis of the growth of

a precipitate is much more complicated. Glicksmann evaluated the moving-boundary problem of 3D precipitate growth in relation to the static-boundary case [22], and found that for small supersaturations the difference is negligible. A similar analysis has been done by Aaron and coworkers in the context of diffusional phase transformations [23].

The growth of a single precipitate on a relatively large grain boundary has been evaluated by Aaron and Aaronson [16], and by Brailsford and Aaron [24]. Brailsford and Aaron [24] report the growth rate of the precipitate thickness S and the radius R. The volumetric growth rate obtained from this analysis, is equivalent to the filling rate in our analysis ($f \propto t^{\nu}$). In the experimental data of Brailsford and Aaron, this volumetric time exponent of precipitate growth on a grain boundary is between 0.72 and 1.05. Aaron and Aaronson [16] found an experimental volumetric time exponent of 0.85. These results are in excellent agreement with our predicted time exponent for precipitate growth inside creep cavities with a large intercavity distance λ/a on grain-boundaries.

The transition between these two diffusion regimes; one dominated by grain-boundary diffusion and one dominated by bulk diffusion, has been observed by Yi and coworkers [25]. This is related to the depletion of solute from the grain boundary, and subsequently transporting solute from the bulk which can be depleted in later stages of precipitate growth. Yi and coworkers showed that in practical situations, the change in character can play a significant role in growth rate of precipitates on grain boundaries.

The transition between two regimes might have been observed for creep cavity growth as well. When single creep cavities in brass were monitored by Isaac and coworkers using X-ray tomography [26], it was found that the cavity growth rates can change abruptly during the creep life-time.

The diffusional transport character of second phase particles or the growth of creep cavities is very sensitive to the intercavity or interprecipitate distance. For our case of precipitation inside creep cavities, the nucleation of new creep cavities during creep reduces the intercavity distance. This behaviour has implications on the self healing process of creep steels, where the interdistance between creep cavities decreases until coalescence joins them. Precipitates forming on the creep cavity surfaces can grow through 2D grain-boundary diffusion, or in later stages through 1D volume diffusion. The transitions in behaviour are mapped and can thereby be predicted.

5. Conclusions

The filling of creep cavities located on grain boundaries perpendicular to the applied stress, through the diffusional flux of supersaturated solute is modelled using finite element methods. The time required for filling depends on the volume diffusivity D_V and grain-boundary diffusivity D_{gb} and on the intercavity spacing λ with respect to the creep cavity size a. For a relatively fast grain-

boundary diffusivity the geometric factor λ/a determines whether the solute can be drained from the grain boundary, or has to come primarily from the bulk. For a relatively large intercavity spacing 3D transport is observed when the grain boundary and volume diffusivities are of a similar order of magnitude, while a 2D behaviour is observed when the grain boundary diffusivity is dominant. Instead, when the intercavity distance is small, the transport behaviour tends to a 1D behaviour in all cases, as the amount of solute available in the grain boundary is insufficient. The various regimes could be identified when the normalised time for creep cavity filling was analysed with respect to the intercavity distance and the diffusivity ratios. The kinetics of the filling fraction for 1D transport scales as $f \propto t^{0.5}$, while for 2D and 3D transport an effective scaling of approximately $f \propto t^{0.85}$ is observed. Predictions are provided for the transitions between the three regimes. The three regimes identified and the transition between the regimes, are experimentally found in applications where precipitation growth or creep cavity growth is observed. The accurate prediction of this regime change is important for the correct description of the growth of second phase particles or creep cavities, during long service lives.

Acknowledgements

We gratefully acknowledge the help of Fred Vermolen and Guus Segal with the software package Sepran. We thank Ekkes Brück, Sybrand van der Zwaag and Haixing Fang for fruitful discussions.

Disclosure statement

No potential conflict of interest was reported by the authors.

Funding

This research is financially supported by the innovation-oriented research program (IOP) on self-healing materials of the Dutch Ministry of Economic Affairs, Agriculture and Innovation [project number SHM012011].

References

[1] F. Abe, T. Kern, and R. Viswanathan, *Creep-resistant Steels*, Woodhead Publishers, Boca Raton, FL, 2008.
[2] K. Maruyama, K. Sawada, and J. Koike, *Strengthening mechanisms of creep resistant tempered martensitic steel*, ISIJ Int. 41 (2001), pp. 641–653.
[3] K. Laha, J. Kyono, S. Kishimoto, and N. Shinya, *Beneficial effect of B segregation on creep cavitation in a type 347 austenitic stainless steel*, Scripta Mater. 52 (2005), pp. 675–678.
[4] N. Shinya, *Self healing of mechanical damage in metallic materials*, AST 54 (2008), pp. 152–157.
[5] E.G. Karpov, M.V. Grankin, M. Liu, and M. Ariyan, *Characterization of precipitative self-healing materials by mechanokinetic modeling approach*, J. Mech. Phys. Solids. 60 (2012), pp. 250–260.

[6] S. Zhang, C. Kwakernaak, W.G. Sloof, E. Brück, S. Van Der Zwaag, and N.H. Van Dijk, *Self healing of creep damage by gold precipitation in iron alloys*, Adv. Eng. Mat. 17 (2015), pp. 598–603.
[7] S. Zhang, C. Kwakernaak, F.D. Tichelaar, W.G. Sloof, M. Kuzmina, M. Herbig, D. Raabe, E. Brück, S. van der Zwaag, and N.H. van Dijk, *Autonomous repair mechanism of creep damage in Fe–Au and Fe–Au–B–N alloys*, Met. Mat. Trans. A 46 (2015), pp. 5656–5670.
[8] S. Zhang, H. Fang, M.E. Gramsma, C. Kwakernaak, W.G. Sloof, F.D. Tichelaar, M. Kuzmina, M. Herbig, D. Raabe, E. Brück, S. van der Zwaag, and N.H. van Dijk, *Autonomous filling of grain-boundary cavities during creep loading in Fe–Mo alloys*, Met. Mat. Trans. A 47 (2016), pp. 4831–4844.
[9] H. Fang, C.D. Versteylen, S. Zhang, Y. Yang, P. Cloetens, D. Ngan-Tillard, E. Brück, S. van der Zwaag, and N.H. van Dijk, *Autonomous filling of creep cavities in Fe–Au alloys studied by synchrotron X-ray nano-tomography*, Acta Mat. 121 (2016), pp. 352–364.
[10] W.W. Sun, H. Fang, N.H. van Dijk, S. van der Zwaag, and C.R. Hutchinson, *Linking surface precipitation in Fe–Au alloys to its self-healing potential during creep loading*, Met. Mat. Trans. A 48 (2017), pp. 2109–2114.
[11] C. Herring, *Diffusional viscosity of a polycrystalline solid*, J. Appl. Phys. 21 (1950), pp. 437–445.
[12] D. Hull and D.E. Rimmer, *The growth of grain-boundary voids under stress*, Phil. Mag. 4 (1959), pp. 673–687.
[13] A. Needleman and J.R. Rice, *Plastic creep flow effects in the diffusive cavitation of grain boundaries*, Acta Metall. 28 (1980), pp. 1315–1332.
[14] E. van der Giessen, M.W.D. van der Burg, A. Needleman, and V. Tvergaard, *Void growth due to creep and grain boundary diffusion at high triaxialities*, J. Mech. Phys. Sol. 43 (1995), pp. 123–165.
[15] C. Zener, *Void growth due to creep and grain boundary diffusion at high triaxialities*, J. Appl. Phys. 20 (1949), pp. 950–953.
[16] H.B. Aaron and I.H. Aaronson, *Growth of grain boundary precipitates in Al-4% Cu by interfacial diffusion*, Acta Metall. 16 (1968), pp. 789–798.
[17] H.B. Aaron and G.R. Kotler, *Second phase dissolution*, Metall. Trans. 2 (1971), pp. 393–403.
[18] H.I. Aaronson, M. Enomoto, and J.K. Lee, *Mechanism of Diffusional Phase Transformations in Metals and Alloys*, CRC Press, Boca Raton, FL, 2010.
[19] A. van den Berg, G. Segal, and D.A. Yuen, *SEPRAN: A versatile finite-element package for a wide variety of problems in geosciences*, J. Earth. Sci. 26 (2015), pp. 89–95.
[20] G. Segal, *The SEPRAN Package*. Available at http://ta.twi.tudelft.nl/sepran/sepran.html.
[21] R. Raj and M.F. Ashby, *Intergranular fracture at elevated temperature*, Acta Metall. 23 (1975), pp. 653–666.
[22] M.E. Glicksman, *Diffusion in Solids: Field Theory, Solid-State Principles, and Applications*, Wiley, New York, 1999.
[23] H.B. Aaron, D. Fainstein, and G.R. Kotler, *Diffusion-limited phase transformations: A comparison and critical evaluation of the mathematical approximations*, J. Appl. Phys. 41 (1970), pp. 4404–4410.
[24] A.D. Brailsford and H.B. Aaron, *Growth of grain-boundary precipitates*, J. Appl. Phys. 40 (1969), pp. 1702–1710.
[25] G. Yi, M.L. Free, Y. Zhu, and A.T. Derrick, *Capillarity effect controlled precipitate growth at the grain boundary of long-term aging Al 5083 alloy*, Metall. Mater. Trans. A 45 (2014), pp. 4851–4862.

[26] A. Isaac, K. Dzieciol, F. Sket, and A. Borbely, *In-situ microtomographic characterization of single-cavity growth during high-temperature creep of leaded brass*, Metall. Mater. Trans. A 42 (2011), pp. 4851–4862.
[27] J. Crank, *The Mathematics of Diffusion*, Oxford University Press, Oxford, 1975.

Appendix 1. Ideal solutions to 3D, 2D and 1D diffusion problems

The mass flux of solute in a medium depends for a large part on the geometry of the problem. Of particular interest for creep cavity filling is the time dependence of the flux at the edge of the creep cavity. In this appendix the time dependence of this flux is evaluated for ideal 3D, 2D and 1D solute transport.

A.1. 3D solute transport

For a spherical cavity and isotropic diffusion ($D_{gb}/D_V = 1$) without boundaries ($\lambda/a \rightarrow \infty$), the problem has been treated analytically [22]. For a constant diffusivity we can start from the diffusion equation in spherical coordinates;

$$\frac{\partial c}{\partial t} = D_V \left(\frac{\partial^2 c}{\partial r^2} + \frac{2}{r} \frac{\partial c}{\partial r} \right). \tag{A1}$$

For a static position of the boundary of the creep cavity ($r = a$) the concentration profile takes the following form [22],

$$\frac{c_0 - c(r,t)}{c_0 - c_1} = \frac{a}{r} \operatorname{erfc} \left(\frac{r-a}{2\sqrt{D_V t}} \right) \quad \text{for} \quad r \geq a. \tag{A2}$$

The solute flux at the edge of the creep cavity $J(r = a) = -(D_V/\Omega)(\partial c/\partial r)$, determines the filling rate of the creep cavity. The development of the concentration profile determines the diffusional flux at the edge boundary resulting in

$$J(a) = -\frac{D_V \Delta c}{a\Omega} \left(1 + \frac{a}{\sqrt{\pi D_V t}} \right) = -\frac{D_V \Delta c}{a\Omega} \left(1 + \frac{1}{\sqrt{\pi \tau}} \right). \tag{A3}$$

where $\Delta c = c_0 - c_1$. For short times ($\tau \ll 1/\pi$), the second term, which represents 1D diffusion, prevails. This is logical as the diffusion length is short with respect to the cavity radius for short times. For longer times ($\tau \gg 1/\pi$) the steady-state growth of a precipitate proceeds as follows,

$$J(a) \approx -\frac{D_V \Delta c}{a\Omega} \quad \text{for} \quad \tau \gg \frac{1}{\pi} \tag{A4}$$

The filling fraction is now obtained after integration of the flux over surface area and time. In the initial stage ($\tau \ll 1/\pi$) the time exponent for the filling fraction $f \approx t^{\nu}$ is $\nu = 0.5$. In the later stages of filling the dominant time exponent for the filling fraction ($f \propto t^{\nu}$) for isotropic 3D diffusion is $\nu = 1$. In practical cases $0.5 \leq \nu \leq 1$ can be found.

A.2. 2D solute transport

For a cylindrical cavity and isotropic grain-boundary diffusion without boundaries ($\lambda/a \rightarrow \infty$), the 2D diffusion equation corresponds to [22]

$$\frac{\partial c}{\partial t} = D_{gb} \left(\frac{\partial^2 c}{\partial r^2} + \frac{1}{r} \frac{\partial c}{\partial r} \right). \tag{A5}$$

The concentration profile is mathematically complex, but relatively quickly approaches an equilibrium shape. For this equilibrium situation $\partial c/\partial t = 0$, providing a general solution to the concentration profile of the form [27]

$$c(r) = A + B\ln(r). \tag{A6}$$

With boundary condition $c(r = a) = c_1$ and $c(r = \lambda) = c_0$, the concentration profile becomes [27]

$$c(r) = \frac{c_1 \ln(\lambda/r) + c_0 \ln(r/a)}{\ln(\lambda/a)}. \tag{A7}$$

The flux at the creep cavity surface is then;

$$J(a) = -\frac{D_{gb}\Delta c}{a\Omega}\frac{1}{\ln(\lambda/a)}. \tag{A8}$$

This flux corresponds to the solution for long times (steady-state). For short times, the diffusion length is small compared to the cavity radius, and in analogy to the case for 3D diffusion, the diffusional flux should effectively be 1D in nature, with $J(a) = -(D_{gb}\Delta c/\Omega\sqrt{\pi D_{gb}t})$. The filling fraction is obtained after surface and time integration of the flux. The dominant time exponent for the filling fraction ($f \propto t^{\nu}$) for isotropic 2D diffusion is $\nu = 1$ in the later stages of filling, as can be seen from Equation (A8). For short times $\nu = 0.5$ is expected. In practical cases $0.5 \leq \nu \leq 1$ can be found. The cross-over between the solution for short and long times is expected to take place when $2\sqrt{D_{gb}t} \approx a$, which leads to $\tau \approx (1/4)(D_v/D_{gb})$.

The flux rapidly stabilises to a constant value, which is similar to the case of 3D symmetric cavity filling. This solution is similar to the simplified solution of Herring [11], describing the axial diffusional growth of creep cavities, which means that like the 3D case, the time exponent for the diffusional flux tends to $\nu = 1$ for large times.

A.3. 1D solute transport

In planar geometry (1D), the diffusion equation corresponds to;

$$\frac{\partial c}{\partial t} = D_V\left(\frac{\partial^2 c}{\partial r^2}\right). \tag{A9}$$

The well-known concentration profile, for boundary conditions $c(r = a) = c_1$ and $c(r = \lambda) = c_0$, is of the form

$$\frac{c_0 - c(r,t)}{c_0 - c_1} = \operatorname{erfc}\left(\frac{r-a}{2\sqrt{D_V t}}\right). \tag{A10}$$

The flux at the edge of the creep cavity is now

$$J(a) = -\frac{D_V\Delta c}{\Omega}\frac{1}{\sqrt{\pi D_V t}} = -\frac{D_V\Delta c}{a\Omega}\frac{1}{\sqrt{\pi\tau}}. \tag{A11}$$

The filling fraction is obtained after surface and time integration of the flux. The time exponent for the filling fraction ($f \propto t^{\nu}$) for 1D diffusion is always $\nu = 0.5$.